Seepage Evaluation in Embankment Dam based on Short-term Temperature Observation and Heat Injection

Bui Quang Cuong
China Three Gorges University, Yichang, Hubei 443002, China
e-mail: cuongvlxd@tlu.edu.vn

Zhou Yihong
China Three Gorges University, Yichang, Hubei 443002, China
Corresponding author e-mail: zyhwhu2003@163.com

Zhao Chunju
China Three Gorges University, Yichang, Hubei 443002, China
e-mail: Chunju.zhao@163.com

ABSTRACT

This research proposes a method for estimating seepage in embankment dam based on short-term temperature observation in condition of heat injection. An actual segment of embankment dam is simulated with a set of various thermal-hydraulic parameters in order to bring effects of these factors on concurrent thermal and seepage transportation through embankment dam to light. The results from numerical modeling indicate that among many factors used for this simulation just some of them have significant influence on process of thermal and seepage propagation. Furthermore, the effect of thermal conductivity variation just clearly happens in small space surrounding heat source, while the alteration of volumetric heat capacity causes a larger incidence. And when seepage velocity go up a threshold (large enough) the redistribution of temperature strongly occur specially toward downstream. By analyzing the results, authors confidently affirm that it is absolutely available to use short-term temperature measurement to evaluate seepage in embankment dam. Moreover, the using of short-term temperature monitoring also creates great benefit, it can reduce the cost and time of surveillance and make the method more attractive.

KEYWORDS: Short-term temperature observation; thermal-hydraulic parameters; heat injection; thermal and seepage.

INTRODUCTION

Various statistics of dam failures uniformly indicate that failures of embankment dam occupy majority in total (more than 65 percent). Furthermore, among reasons causing embankment dam failure, seepage/erosion accounts for significant proportion (approximate 40 percent). Some statistics illustrating for dam failure data can be found in (Zhang et al., 2007, You et al., 2012, Pyayt et al., 2013). Most dam failures relating to seepage problems is either caused by lacking of monitoring system or had monitoring system but it was out of order (Johansson, 1997). All the aforementioned problems obviously show that seepage observation for embankment dam is a crucial task which promotes efficiency and safety of projects during operation.

Among various methods, seepage evaluating from temperature data has been expressing as a feasible method which could give real time information of seepage condition. The method development are commonly considers in two aspects, one is analytic method and the other is temperature monitoring technologies. For the former, seepage evaluation from temperature data can be divided into two categories based on the length of time monitoring. Short-term

observations are usually applied to detect leakage regions, while long-term surveillances can be used to estimate seepage velocity. The later one, temperature monitoring technologies are classified by either types of equipment or measuring method.

Regarding evaluation of seepage velocity, a vast number of studies applied numerical modelling to analyze concurrent thermal and seepage in soil medium, several typical researches in this field from 1960s to 1980s are (Stallman, 1965, Cartwright, 1968, Cartwright, 1974, Sorey, 1971, Domenico and Palciauskas, 1973, Birman, 1968, Smith and Chapman, 1983). Despite these researches is not developed far enough to serve as orthodox method for leakage detection in embankment dam, they contribute as the basic foundation for post-studies. In recent two decades the method has been strongly developing with support of advanced technology in temperature measurement as well as the development of analytic approaches. Commonly, by the way of numerical modelling, various soil thermal-hydraulic parameters are employed to compute concurrent temperature and seepage in dam, then the expected temperatures from numerical solutions were compared with temperature measurements to find out the closest result. From which seepage velocity were determined. Interested readers can find more detail information in (Johansson, 1997, Smith and Konrad, 2008, Shija and MacQuarrie, 2015, S. Yousefi, 2013, Velásquez, 2007).

The main limitation of previous researches are the application of passive method which observes changing of internal temperature affected by nature external thermal loads (air temperature, water temperature, geothermal), this led to long time observation demanding. Besides, the using of average temperature (weekly or monthly) for numerical modelling somewhat does not reflect the actual condition of temperature and seepage inside the dam. To overcome these limitations the application of heat-pulse method also known as active method is a good solution (Dornstädter and Geophys, 2013). The active method was employed in several researches, for instant (Beck et al., 2010, Dornstädter and Geophys, 2013), however, these research only concentrated to explore the presence of leakage regime, even they can give the information of seepage condition but it just was qualitative seepage intensity without quantitative seepage velocity.

In order to fill up the aforementioned void, this present work use numerical modelling to analyze seepage and temperature distribution in embankment dam with complement of active heat injection method in short-term temperature data. An actual dam was simulated with different soil hydraulic-thermal parameters, whereby the influences of these parameter on seepage and temperature behavior are elucidated. Moreover, a supposition suffusion layer within the dam was made so as to investigate the effect of suffusion layer on temperature distribution.

BASIC THEORY

In field of coupled thermal-seepage analyses, the solution of conservative principals usually is simplified by adding hypotheses. Interested readers are referred to publications by (Johansson, 1997, Domenico and Palciauskas, 1973, Diersch and Kolditzb, 1998, Velásquez, 2007, Radzicki and Bonelli, 2010, DHI-Wasy, 2009). Flowing DHI-Wasy (2009) with hypotheses: 1. Fluid is incompressible substance; 2. Water movement in soil is laminar flow; 3. There is no temperature difference between soil and water at local points; 4. Effects of air and water vapor in thermal processes are neglected; 5. Soil deformation is ignored; Heat and water transport in variable saturated soil can be denoted as Eq.1, Eq.2.

$$\begin{gathered}\left[s^f \varepsilon \rho^f c^f + (1-\varepsilon)\rho^s c^s\right]\frac{\partial T}{\partial t} + \rho^f c^f q \nabla T \\ -\nabla\left[\left(s^f \varepsilon \lambda^f I + (1-\varepsilon)\lambda^s I + \varepsilon \rho^f c^f D_m\right)\nabla T\right] + \varepsilon \rho^f c^f \overline{Q}_\rho (T - T_o) \\ -\varepsilon \rho^f \overline{Q}_T^f + (1-\varepsilon)\rho^s \overline{Q}_T^s = 0\end{gathered} \tag{1}$$

$$q = -K_r(s^f)Kf_\mu\left(\nabla h + \frac{\rho^f - \rho_o^f}{\rho_o^f}e\right) \quad (2)$$

And constitutive relationships

$$h = \frac{\rho^f}{\rho_o g} + z = \Psi + z \quad (3)$$

$$K = \frac{k\rho_o^f g}{\mu_o^f} \quad (4)$$

$$f_\mu = \frac{\mu_o^f}{\mu^f(T)} \quad (5)$$

where: s^f- Saturation (dimensionless); ε- Porosity (dimensionless); ρ^f, ρ^s- density of fluid and soil, [ML^{-3}]; c^f, c^s- specific heat capacity of fluid and soil, [$L^2T^{-2}K^{-1}$]; T- Temperature, [K]; t- Time, [T]; q- Darcy flux vector, [LT^{-1}]; $\lambda^f \lambda^s$- Thermal conductivity of fluid and soil, respectively, [$MLT^{-3}K^{-1}$]; I- Unit vector; D_m- Tensor of mechanical dispersion, [L^2T^{-2}]; $\overline{Q}_\rho$- Average fluid mass sink/source, [T^{-1}]; $\overline{Q}_T^f, \overline{Q}_T^s$- Average heat sink/source of fluid and soil, [$ML^{-1}T^{-3}$]; h- Hydraulic head, [L]; K Tensor of hydraulic conductivity, [LT^{-1}]; k- Intrinsic permeability, [m^2]; μ_o^f, μ^f-Reference dynamic viscosity and dynamic viscosity of fluid, [$ML^{-1}T^{-1}$]; ρ_o^f- Reference fluid density [ML^{-3}]; e- Gravitational unit vector; g- Gravitational acceleration [LT^{-2}]. K_r- Relative hydraulic conductivity, (dimensionless). $0 < K_r \leq 1, K_r = 1\ when\ s^f = 1$, and operator ∇ stand for $\left(\frac{\partial}{\partial x} + \frac{\partial}{\partial y} + \frac{\partial}{\partial z}\right)$.

K_r, and s^f are usually specified by empirical relationship relating to pressure head. Some popular models using to estimate these parameters such as Genuchten-Mualem model, Brooks-Corey model, and Havekamp model (Boufadel et al., 1999, DHI-Wasy, 2009). Following Genuchten-Mualem model it is stated that:

$$s_e^f = \begin{cases} \dfrac{1}{[1 + |A\Psi^n|]^m} & \text{for } \Psi < 0 \\ 1 & \text{for } \Psi \geq 0 \end{cases} \quad (6)$$

$$K_r = \left(s_e^f\right)^{1/2}\left[1 - \left(1 - \left(s_e^f\right)^{1/m}\right)^m\right]^2 \quad (7)$$

$$s_e^f = \frac{s^f - s_r^f}{s_s^f - s_r^f} = \frac{\theta^f - \theta_r^f}{\theta_s^f - \theta_r^f} \quad (8)$$

where: s_s^f, s_r^f: Maximum and residual saturation of fluid, [fluid volume per void volume]; $\theta^f, \theta_s^f, \theta_r^f$: Volumetric moisture content, saturated volumetric moisture content and residual volumetric moisture content, respectively [rate of water volume and bulk volume] ; A and n: Genuchten-Mualem fitting parameters.

GENERAL DESCRIPTION

Aim to make the research closes with reality, an actual geometry of a dam locating in the middle of Vietnam was selected for numerical simulation. Representative cross-section of the dam is sketched as in figure 1.

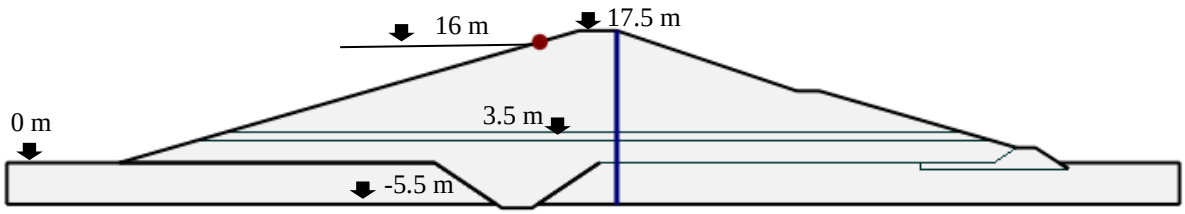

Figure 1: Representative cross-section of the Dam.

The dam is constructed by homogeneous soil with the drainage in downstream. The dam height is 17.5 m, and dam crest width is 5 m. The upstream slope gets value of 3.5, while the downstream slope is separated into two parts at elevation of the berm, values of downstream slope are 3 and 3.5 corresponding to upper and lower part. The dam is constructed above foundation having higher hydraulic conductivity (comparing with hydraulic conductivity of the dam), and the width of the foundation is just 5.5 m, therefore, a cut-off trench used the same material as in main dam was constructed through the foundation in order to prevent high seepage velocity go through the foundation. In addition, to apply active heat injection method, an assumed standpipe was disposed in the edge of dam crest and it go through the dam and foundation. Other standpipe can be also set up to observe temperature in adjacent medium of the heat source. In reality, the exiting standpipe using for seepage observation should be utilized so as to economize as well as minimize the bad effects of standpipe arrangement's process to the dam. In case of new stand pipe setting, the application of Jürgen Dornstädter's method that rams array of small diameter metallic tubes into soil, temperature is recorded along the tubes when temperature of tubes were equal with surrounding temperature. This method is cost-effective for embankment dam with height from 20 to 30 m (Dornstädter and Geophys, 2013, Johansson, 1997).

Normally, concurrent heat and water transfer in embankment dam can be simulated in problem of two dimensions to reduce computing time and computer space consumption as well. However, the application of line heat source in standpipe cannot be distributed along dam (because of the limitation of standpipe) so obviously the effect of heat source to temperature variation at different position is not the same. Therefore, in case of line heat source model the application of three dimension simulation is necessary.

To investigate the efficiency of the method twelve scenarios was attempted. Results from computation shows that the effect of heat source to temperature distribution in transversal direction to adjoining media was limited at distance of 4 m, therefore a 12 m dam segment generated based on the representative cross-section was selected for simulation. As can be seen from figure 2 the line heat source is disposed inside the model at the distance of 4.0 m from right side of the model. In vertical direction line heat source just be applied in scope of seepage which was calculated from stable stage.

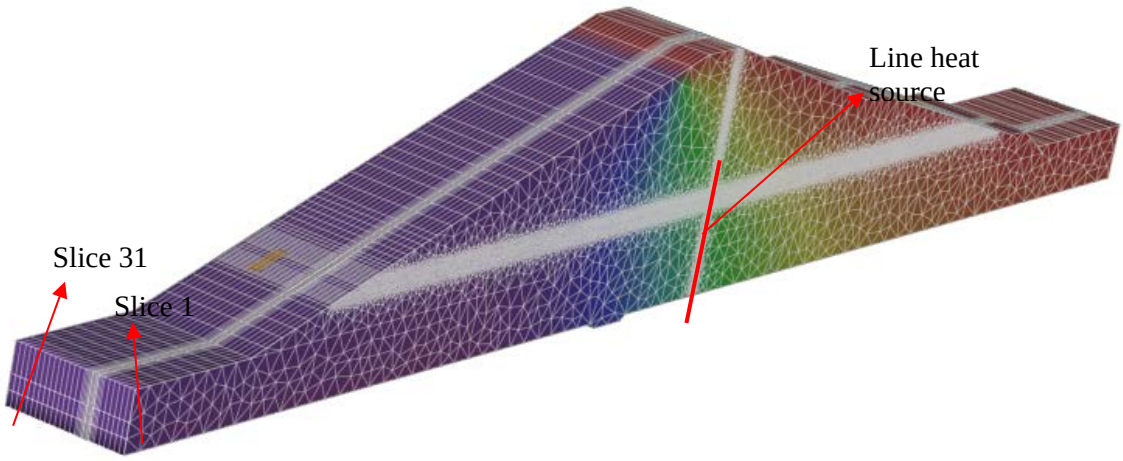

Figure 2: Three dimensions geometry of the dam segment used for simulation

COUPLED MODELLING OF SEEPAGE AND TEMPERATURE TRANSPORT IN EMBANKMENT DAM

Numerical Model Selection

Coupled thermal and seepage transfer in soil medium are very complex processes, it usually cannot obtain the solution by manual calculation. Therefore, a numerical model paying role as working tool is necessary. Currently, many software are available to solve the problem of coupled thermal-fluid transportation through earthen structure, for examples FEFLOW, ANSYS, GEOSTUDIO, TOUCH2, SUTRA, COMSOL and so on. After analyzing these software's capabilities, the FEFLOW code developed by WASY GmBH was selected because: 1. the code is specially designed for modelling of water movement in soil media. 2. Coupled modelling of thermal and seepage transport in saturated/unsaturated soil medium is available for both of steady and transient state. 3. The problem with complex boundary conditions and geometries can be solved with robustness of numerical methods. 4. It includes flexible schemes for time step control. 5. It was previously used to solve the problem of concurrent thermal seepage transfer in porous media, for instance see (Velásquez, 2007, Shija and MacQuarrie, 2015).

Parameters Use for Numerical modelling

By using FEFLOW to simulation concurrent heat and mass transfer in soil medium, a set of soil thermal-hydraulic parameters need to be supplied. With the purpose of investigating the effect of each parameter (soil thermal-hydraulic parameters) on heat and seepage transportation through an embankment dam, an original scenario is firstly computed with a specific set of parameters, then each parameter in the set is altered to get new scenarios. Subsequently, the result of new scenarios are compared with the original one (the result of the first scenario). From which the effect of these parameters is determined.

Soil thermal-hydraulic properties show very broad ranges of variation, they depend on many factors for example constitution of soil, saturation, temperature, grain size and so on, therefore, it is unfeasible to carry out all these ranges of soil properties in one research. This research first of all takes the real values of soil hydraulic parameters comprising porosity, saturated hydraulic conductivity, soil constitution, grain size from the project's report as in the first scenario. Afterward, based on the type of known soil, literatures relating to properties of typical soil for homogeneous embankment dam, the missed soil thermal-hydraulic parameters was studied and complemented to build up twelve scenarios as expressed in table 1. Literatures used to constitute table 2 include (Yu et al., 1993, Novak et al., 2007, Kestin et al., 1978, Shao and Horton, 1998) and (Abu-Hamdeh, 2003, Hamdhan and Clarke, 2010, Gori and Corasaniti, 2013, Nikiforova et al., 2013) for soil hydraulic and soil thermal properties, respectively.

Numerical Model Implementation

Meshing

FEFLOW provides unstructured triangular mesh which is extremely fast meshing tool for 2D complex geometry, moreover, the meshing tool permitting to refine mesh in selected line or point, this supply a flexible solution for users. Besides, layer-based approach, a structured meshing algorism, permit users easily extend 2D problem to 3D simulation.

In the present work, first of all an unstructured triangular mesh was designed for typical dam cross-section, where the position of line heat source was specified. According to results from simulation, authors found out that element closing with heat source and suffusion layer need to small enough (size of element is not lager than 0.3) to give a precise solution, therefore, at the position the mesh was refined to meet the requirement. Afterward, slices with the same features of principle 2D mesh were generated by using 3D configuration tab. In general, the distance between two slices is 0.5 m, however, as mentioned above, at position of line heat source distance between

two slices was reduced to 0.2 m. Finally, a 3D mesh of the dam segment with 31 slices was generated as in fig.2.

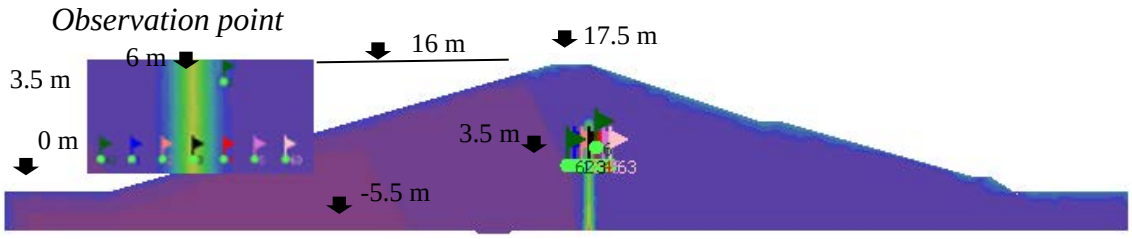

Figure 3: Arrangement of observation point in slice 12

With purpose of investigation the efficiency of the line heat source, a set of observation point was arranged in the numerical model. Beginning with slice 12 (4 m far away from the first slice), observation points 1, 2, 3, 4, 5, 6, 62, 63 were set at elevation 3.5 m, where pair of observation points 62, 63; 1, 5; 2, 4 are symmetric about line heat source, the distance from point 62, 1, 2 to the heat source is 3 m, 2 m, 1 m, respectively. Observation point 3 was located at adjacent position of line heat source, whereas, point 6 is the same coordinate in x and y direction with point 4 but at elevation 6 m. The observation points then continuously set on slices 17, 19, 21, 23, 25, 27, 29, 31 in the same way of observation points 1, 2, 3, 4, 5, 6 in slice 12.

Boundary condition

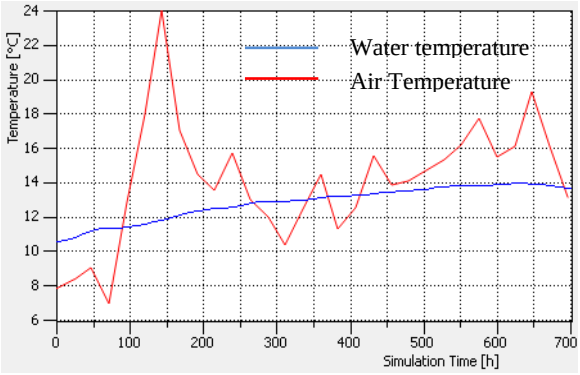

Figure 4: Temperature boundary conditions

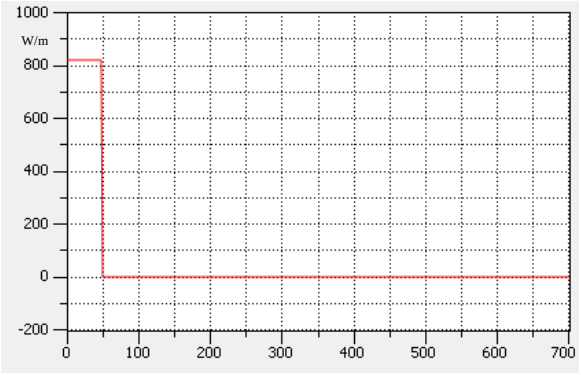

Figure 5: Line heat source boundary condition

Reality shows that air temperature observation in short-term does not conform to any rule, therefore, the best solution is to apply the real temperature monitored in the dam surfaces. However, Because there is no available data from the project, so this research used temperature variation of air and water in August, 1997 (see figure 4) subtracted from data of (Smith and Konrad, 2008). Because this is a general research thus the application of this temperature boundary condition does not reduce the rule of generality. Besides, a constant heat injection rate of 820 W/m was uniformly assigned along standpipe's entire length in 2 days period. Continuously, a constant geothermal heat flux with value of 0.16 W/m^2 was employed for temperature boundary condition of foundation.

Regarding the hydraulic boundary condition, the constant head with value 16 m and 0 m corresponding to upstream and downstream was applied. Actually, the water level in reservoirs is fluctuation, nevertheless, with short-time simulation the amplitude of oscillation is small so the steady water head in upstream boundary is acceptable.

Table 1: Parameters Use for Numerical Modelling

Group	Factors	unit	Scenarios											
			1	2	3	4	5	6	7	8	9	10	11	12
Initial conditions	Water distribution	m	From results of steady state											
	Temperature distribution	^{o}C	From results of steady state											
Boundary conditions	Geothermal	$W.m^{-2}$	0.065											
	Heat injection	$W.m^{-1}$	820 (in the first 48 hours)											
	Temperature of water	^{o}C	Data in August											
	Temperature of air	^{o}C	Data in August											
	Hydraulic head of upstream	m	16											
	Hydraulic head of downstream	m	0											
Fluid flow	Porosity	-	0.35	0.4	x	x	x	x	x	x	x	x	x	x
	Dam Saturated hydraulic conductivity	$m.s^{-1}$	3.0E-08	x	3.0E-06	3.0E-07	x	x	x	x	x	x	x	x
	Foundation Saturated hydraulic conductivity	$m.s^{-1}$	4.0E-07											
	Dynamic viscosity	Pa.s	$\mu^f(T) = 2.414 \times 10^{-2} \times 10^{\frac{247.8}{T-140}}$											
	Genuchten-Mualem fitting parameter A	1/m	1.51	x	x	x	5.0		x	x	x	x	x	x
	Genuchten-Mualem fitting parameter n	-	1.3	x	x	x	x	1.6	x	x	x	x	x	x
	Maximum saturation	-	1.0											
	Residual saturation	-	0.003	x	x	x	x	x	0.3	x	x	x	x	x
Heat transport	Effective porosity	-	0.3	x	x	x	x	x	x	0.2	x	x	x	x
	Thermal conductivity of fluid	$J.m^{-1}.s^{-1}.K^{-1}$	0.65											
	Thermal conductivity of solid	$J.m^{-1}.s^{-1}.K^{-1}$	3	x	x	x	x		x		2.0	4.0	x	x
	Volumetric heat capacity of fluid	$MJ.m^{-3}.K^{-1}$	4.2											
	Volumetric heat capacity of solid	$MJ.m^{-3}.K^{-1}$	3.1	x	x	x	x	x	x	x	x	x	2.0	x
	Longitudinal dispersivity	m	1	x	x	x	x	x	x	x	x	x	x	0.1
	Transversal dispersivity	m	0.1	x	x	x	x	x	x	x	x	x	x	0.01

Note: "x" means the value of that cell is the same with the value of Scenario 1 (the original senario)
"-" Denotes there is no value at that cell

Initial condition

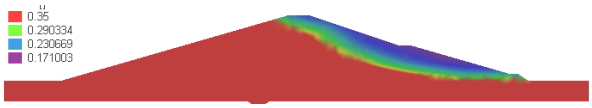

Figure 6:. Initial saturation distribution

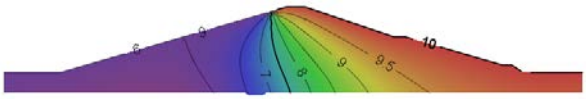

Figure 7. Initial temperature distribution

Initial conditions of thermal-seepage analysis can be assigned to every node by means of global value or regional value with support of interpolation component. However, because of the lack of observation data, therefore the steady state will be computed first, then its results will be applied as initial condition. The initial conditions are shown in figure 6 and figure 7.

RESULTS AND DISCUSSION

First of all we present here the result of the first scenario, from that results of other scenarios will be compared with the original one to point out the effect of soil thermal-hydraulic parameters into seepage and heat transportation in soil medium. In addition, to make a convenience for readers, pairs of temperature distributed curves of symmetrical observation point about line heat source are expressed in the same color but points in upstream are denoted by dash curves while solid curves are employed for downstream point.

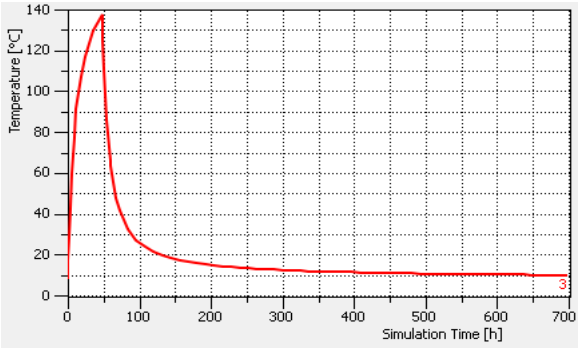

Figure 8. Temperature variation of observation point 3 (scenario 1)

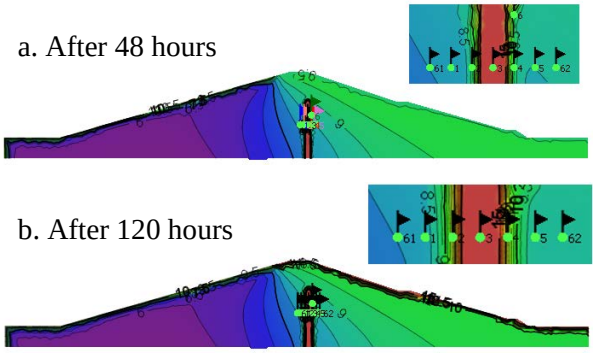

Figure 9. Temperature distribution in slice 12 (Scenario 1)

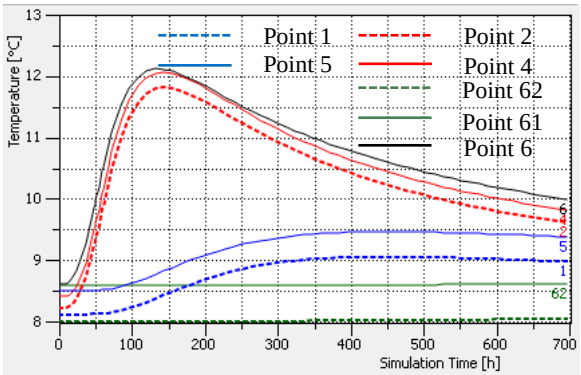

Figure 10. Temperature variation of observation point in longitudinal direction (scenario 1)

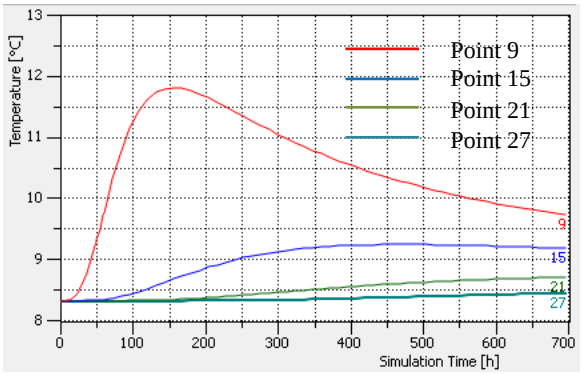

Figure 11. Temperature variation of observation point in transversal direction (scenario 1)

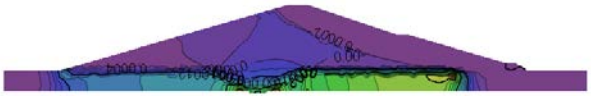

Figure 12: Seepage velocity distribution in slice 5 after 120 hours (scenario 1)

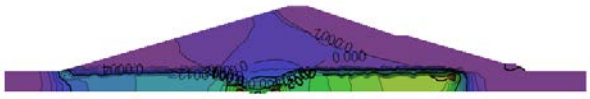

Figure 13: Seepage velocity distribution in slice 5 after 698 hours (scenario 1)

It can be clearly seen from figure 8 that temperature of observation point 3 immediately responds the application of heat source. Dramatically going up in the first 48 hours, Temperature of point 3 tremendously fell down in continuous period from 48 to 80 hours, then the curve gradually decreased and got the value of 10^{o}C at the end of time simulation. Besides, it can be found from figure 9, 10, 11 that the incidence of heat source on surrounding soil was clearly in radius of 2 m, and there was almost no effect at distance of 4 m far away from heat source. Furthermore, temperature of observation points not coinciding with heat source kept stable value around 15 hours and 70 hours for points in distance of 1 m and 2 m, respectively. Afterward, temperature of observation points with distance of 1 m from heat source remarkably grew up and the trend was continuously remained even when the application of heat source stop after 48 hours. Finally, they get their peaks at around 125 hours, then these curves noticeably decreased. For observation points in distance of 2 m from heat source it slowly promoted and get their peak after 350 hours, then the value of temperature at peaks were almost persisted.

Besides, there was no influence of temperature boundary condition comprising air temperature, reservoir temperature, and geothermal in observation points. In one month the effect of water temperature and air temperature was restricted in 4 m from dam surface.

On the other hand, the temperature curves of observation points at the same distance from heat source was parallel, and the temperature difference between upstream and downstream points was small, specially, in position nearby heat source. Furthermore, beginning temperature of point 2 was smaller than temperature of point 4 so when heat source was employed the thermal gradient between heat source and point 2 was bigger, that describes why in the first segment temperature curve of point 2 was a little steeper than point 4. Aforementioned statement lead to a conclusion that thermal transportation in this case was predominated by conduction process.

Regarding to seepage velocity, constant water heads were assigned for up and downstream boundary, in addition, the temperature variation was just in small space surrounding the heat source, therefore, a stable distribution of seepage velocity was endured as shown in figures 12 and 13.

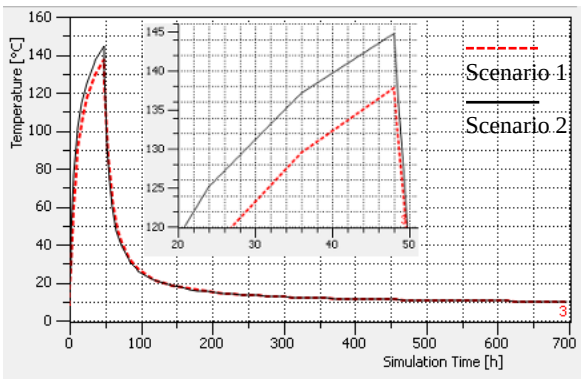

Figure 14: comparison of temperature variation of point 3 between scenario 1 and 2

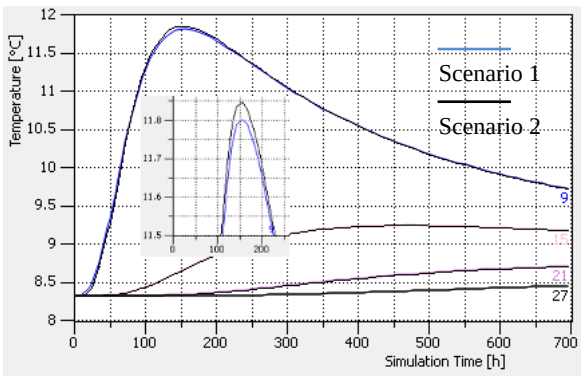

Figure 15: comparison of temperature variation of point 9 to 27 between scenario 1 and 2

Next, the comparison between results of scenarios 2, 5, 6, 7, 12 with scenario 1 was implemented. Because the figures were almost the same, so from now, just representative figures could be used to describe the results. As shown in representative figures 14 and 15, there was only

a significant difference at point 3, for other points they were almost similar. It means that porosity, Genuchten-Mualem fitting parameters, residual saturation, longitudinal and transversal dispersivity in the selected range (table 1) do not affected the concurrent heat and seepage transfer inside the dam.

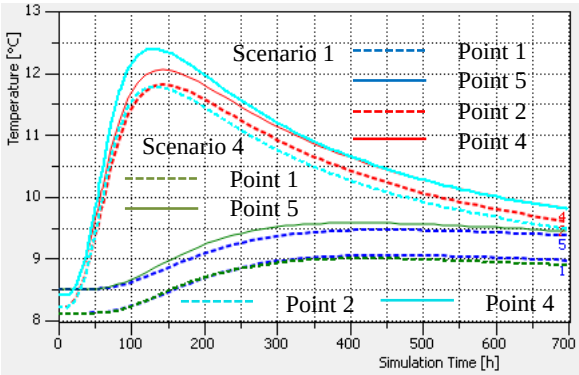

Figure 16: Temperature variation in longitudinal direction of scenario 1 and 4

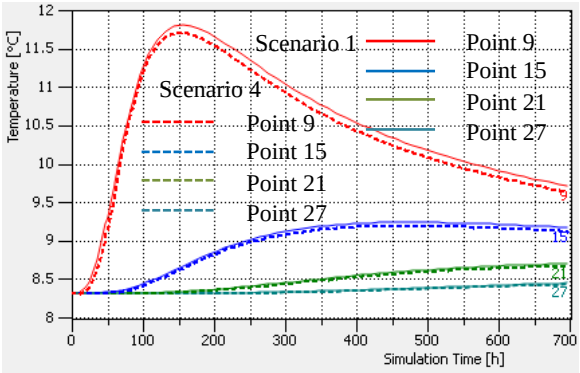

Figure 17: Temperature variation in Transversal direction of scenario 1 and 4

Continuously, result from scenario 4, 8 were compared with the scenario 1, these comparisons showed the small difference between temperature of observation points, and these difference just can be clearly seen at these points in expanse of 1 m. for scenario 4, the increase of hydraulic conductivity caused the enlargement of seepage velocity, this leaded to the development of convection process and made the temperature in upstream fell down and temperature in downstream rose up. However, the growth of seepage velocity was not big enough to create a large difference, the maximum of temperature difference appeared with value a litter smaller than 0.5 ^{o}C. The same with the change of hydraulic conductivity, the decline of effective porosity caused the increase of seepage velocity, it mean that reasoning of scenario 4 is available for scenario 8.

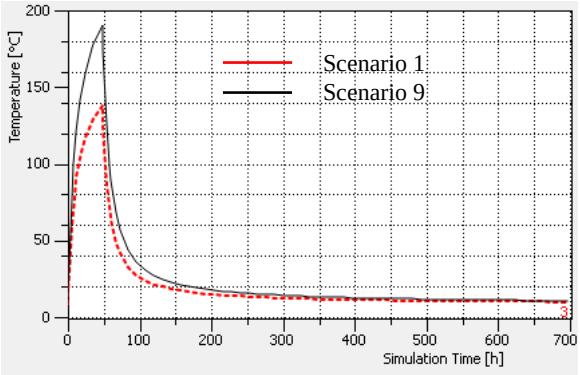

Figure 18: Temperature variation of point 3 in scenario 1 and 9

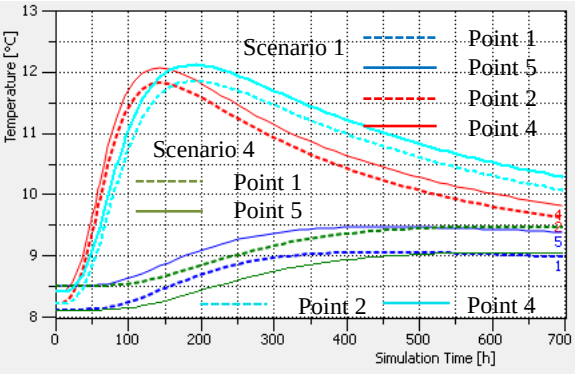

Figure 19: Temperature variation in longitudinal direction of scenario 1 and 9

The reduction of thermal conductivity in scenario 9 slowed down the thermal conduction process, while heat was continuous injected in the model, this made the dissipation process of temperature slower, thus temperature at source margin was higher as presented figure 18. In parallel, the flatter of temperature curves in scenario 9 comparing with the others in scenario 1 described the effect of decrease of thermal conductivity. However, the dissimilarity of temperature between two scenarios just was clearly in margin of heat source, at a distant place, for instance 1 m from heat source the maximum distinction is only slightly higher than 0.5 ^{o}C. The vice versa process is true for scenario 10, which have a rise of thermal conductivity.

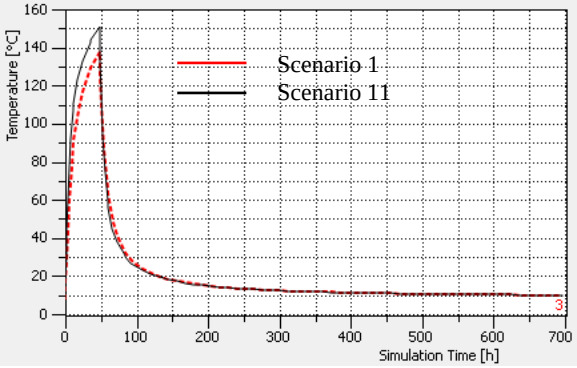

Figure 20: Temperature variation of point 3 in scenario 1 and 11

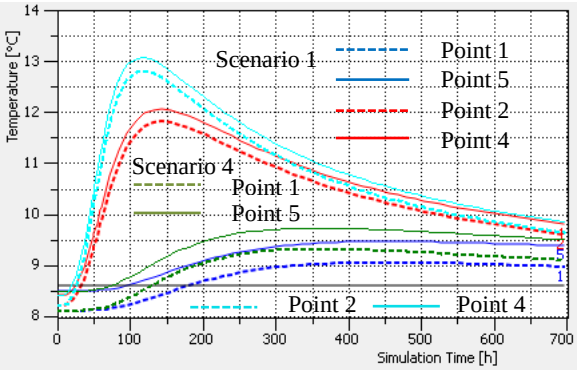

Figure 21: Temperature variation in longitudinal direction of scenario 1 and 11

Figures 20, 21 show that the temperature curves in scenario 11 were steeper than temperature curves in scenario 1, this can be directly explained through the definition of volumetric heat capacity, that soil volumetric heat capacity stands for stored internal energy ability of a given soil volume while undergo a given temperature change. It means that soil with smaller volumetric heat capacity is easier to heat up as well as cool down. In this situation, the effect of the variation generated a larger incidence, there was clear alteration in space of 2 m from heat source.

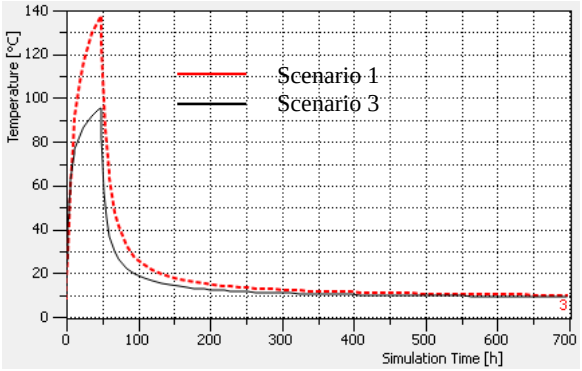

Figure 22: Temperature variation of point 3 in scenario 1 and 3

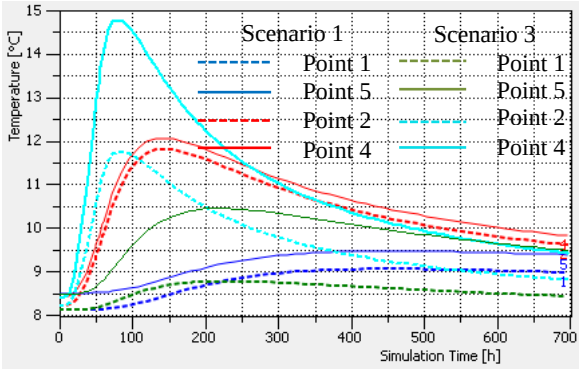

Figure 23: Temperature variation in longitudinal direction of scenario 1 and 3

Based on reasoning that seepage carries heat by itself and exchanges heat with adjacent environment in the way of its movement, thus, it is obvious that temperature in position of heat source is smaller in case of higher seepage velocity because energy from heat source is transmitted to downstream faster by higher seepage velocity (see figure 22). Besides, the velocity in scenario 3 was relatively higher than the one in scenario 1 (0.04 m/d compare with 0.0004 m/d), in this condition, the influence of convection process was quite clear. In the direction toward downstream, the collaboration of temperature transported by seepage (convection process) with temperature caused by conduction process made the temperature in downstream points develop faster and higher as can be seen from figure 23. In contrast, in upstream the convection and conduction process occur in opposite direction, conduction went forward upstream, while convection followed seepage direction. Moreover, in short distance and high temperature gradient, the conduction happened stronger than the convection, furthermore, heat transported by conduction toward upstream was partly carried back by seepage, and it made the energy nearby heat source in upstream part climbed up thus temperature of scenario 3 grew faster than scenario 1 in the first segment as depicted in figure 23, nonetheless, this could to be validate by field experiment. In parallel, the convection process as described above was also the reason make the heat transfer faster toward downstream, therefore, after temperature curves of observation points

in scenario 3 got their peaks, they rapidly slumped down and quickly went to under the temperature curves of scenario 1.

According to results of all scenarios, authors found out that the most valuable information of temperature observation can be gotten after the first 350 hours (around 300 hours after finishing heat injection). Moreover, 48 hours of heat injection is enough for analyzing of concurrent heat and seepage transfer in embankment dam. The reduction of time observation bring about the decline of labor and cost. Additionally, the temperature monitoring system, which is quite expensive, can be alternately used for several projects. Aforementioned things apparently states that the short-term observation make the method more attractive.

CONCLUSIONS

(1) The present work analyzed the transportation process of heat and seepage through an embankment dam based on short-term temperature observation and heat injection. According to the results from scenarios it can be affirmed that seepage can be absolutely evaluated from short-term temperature monitoring, the 2 days of heat injection and 15 days of temperature measurement are enough for seepage estimation.

(2) The results from soil thermal-hydraulic parameters research showed that porosity, Genuchten-Mualem fitting parameters, residual saturation, longitudinal and transversal dispersivity does not significantly affect coupled seepage and thermal propagations in the case study. Besides, the small increase of seepage velocity (hydraulic conductivity) from around 0.0004 to 0.0045 m/d or the decrease of effective porosity give the same trend of temperature increment. However, temperature difference is small, and it just can be explored in radius of 1 m from heat source. The change of thermal conductivity generates the variation of temperature distribution. Nevertheless, there are lager dissimilarly of temperature variation between points, for example, the temperature difference of scenario 1 and scenario 9 at points in heat source adjacent and points locating 1 m far away from heat source are in turn 50 oC and 0.5 oC. Sequence, the variance of temperature in case of decrease volumetric heat capacity have large sphere of influence comparing with the situation of heat conductivity variation, the shifting of volumetric heat capacity causes the smaller temperature variation in heat source adjacent and larger in further distance from heat source than the case of heat conductivity variation. Finally, the role of convection process is clear when seepage velocity is large enough (around 0.035 m/d). In this condition a very clear temperature difference is gotten in both of heat source adjacent and point in distance of 3 m.

(3) The effect of temperature boundary (air temperature, water temperature, and geothermal) condition is limited at around 5 m deep from dam surface for all scenarios, it mean that there is no influence of temperature boundary condition to the analyses of the method.

(4) This paper supplies synthetic and systematic information about basic theory, numerical models of thermal-heat behavior in embankment dam, so that it provides useful information for readers who want to practice or continue to develop the problem.

(5) This work proposed a short-time scheme for seepage estimation from temperature monitoring, it can promote the efficiency of the method.

ACKNOWLEDGEMENTS

The work in this paper is supported by National Natural Science Foundation of China (Grant No. 51479103). The authors would like to appreciate the contribution of colleagues for this research.

REFERENCES

abu-Hamdeh, N. H. 2003. Thermal Properties of Soils as affected by Density and Water Content. *Biosystems Engineering,* 86**,** 97-102.

Beck, y. L., khan, a. A., cunat, p., guidoux, c., artières, o., mars, j. & fry1, J. J. 2010. Thermal Monitoring of Embankment Dams by Fiber Optics. *8th ICOLD European Club Symposium.* Austria: Austrian National Committee on Large Dams.

Birman, J. H. 1968. Leak Detection Method. *United State Patent*.

Boufadel, b. M. C., venosa, a. D., suidan, m. T. & bowers, M. T. 1999. Steady Seepage in Trenches and Dams: Effect of Capillary Flow. *Journal of Hydraulic Engineering,* 125**,** 286-294.

Cartwright, K. 1968. Thermal prospecting for ground water. *Water Resources Research,* 4.

Cartwright, K. 1974. Tracing shallow groundwater systems by soil temperature. *Water Resources Research,* 10.

Dhi-Wasy 2009. *White papers,* Berlin.

Diersch, h.-j. G. & Kolditzb 1998. Coupled groundwater flow and transport: 2. Thermohaline and 3D convection systems. *Advances in Water Resour,* 21.

Domenico, p. A. & Palciauskas, V. V. 1973. Theoretical Analysis of Forced Convective Heat Transfer in Regional Ground-Water Flow. *Geological Society of America Bulletin,* 84**,** 3803-3814.

Dornstädter, J. & Geophys, D. 2013. Leakage Detection in Dams - State of the Art. *20th Anniversary of SLOCOLD.* Ljubljana, Slovakia: Slocold.

GORI, F. & CORASANITI, S. 2013. New model to evaluate the effective thermal conductivity of three-phase soils. *International Communications in Heat and Mass Transfer,* 47**,** 1-6.

HAMDHAN, I. N. & CLARKE, B. G. Determination of Thermal Conductivity of Coarse and Fine Sand Soils. Proceedings World Geothermal Congress 2010, 2010 Bali, Indonesia.

Johansson, S. 1997. *Seepage Monitoring in Embankment Dams.* Doctor, Royal Institute of Technology S-100 44 Stockholm, Sweden.

Kestin, J., Sokolov, M. & Wakeham, A. 1978. Viscosity of Liquid Water in Range -8^{o}C to 150^{o}C. *J. Phys> Chem. Ref. Data,* 7**,** 8.

Nikiforova, T., Savytskyi, M., Limam, K., BOSSCHAERTS, W. & BELARBI, R. 2013. Methods and Results of Experimental Researches of Thermal Conductivity of Soils. *Energy Procedia,* 42**,** 775-783.

Novak, P., Moffat, A. I. B., Nalluri, C. & Narayanan, R. 2007. *Hydraulic Structure,* London, Taylor and Francis.

Pyayt, A. L., Kozionov, A. P., Mokhov, I. I., Lang, B., Krzhizhanovskaya, V. V. & Sloot, P. M. A. 2013. An Approach for Real-time Levee Health Monitoring Using Signal Processing Methods. *Procedia Computer Science,* 18**,** 2357-2366.

Radzicki, K. & Bonelli, S. 2010. Thermal Seepage Monitoring in the Earth Dams with Impulse Response Function Analysis Model. *8th ICOLD European Club Symposium.* Austria.

S. Yousefi, A. N., M. Ghaemian AND S. KHARAGHANI2 2013. Seepage Investigation of Embankment Dams using Numerical Modelling of Temperature Field. *Indian Journal of Science and Technology*.

Shao, M. & Horton, R. 1998. Integral Method for Estimating Soil Hydraulic Properties. *Soil Science Society of America Journal,* 62**,** 8.

Shija, N. P. & Macquarrie, K. T. B. 2015. Numerical Simulation of Active Heat Injection and Anomalous Seepage near an Earth Dam–Concrete Interface. *International Journal of Geomechanics,* 15**,** 04014084.

Smith, L. & chapman, D. S. 1983. On the thermal effects of groundwater flow: 1. Regional scale systems. *Journal of Geophysical Research,* 88**,** 593.

Smith, M. & Konrad, J. M. 2008. Analysis of the annual thermal response of an earth dam for the assessment of the hydraulic conductivity of its compacted till core. *Canadian Geotechnical Journal,* 45**,** 185-195.

Sorey, M. 1971. Measurement of Vertical Groundwater Velocity from Temperature Profiles in Wells. *Water Resources Research,* 7.

Stallman, R. W. 1965. Steady One-Dimensional Fluid Flow in a Semi-Infinite Porous Medium with Sinusoidal Surface Temperature. *JOURNAL OF GEOPHYSICAL RESEARCH,* 70.

Velásquez, J. P. P. 2007. *Further Development of the Gradient Method for Leakage Detection and Localization in Earthen Structures.* Doctor, Technical University of Munich

You, L., Li, C., Min, X. & Xiaolei, T. 2012. Review of Dam-break Research of Earth-rock Dam Combining with Dam Safety Management. *Procedia Engineering,* 28**,** 382-388.

Yu, c., Loureiro, c., Cheng, j.-j., Jones, l. G., Wang, y. Y., Chia, Y. P. & FAILLACE, E. 1993. *Data Collection Handbook to Support Modeling the Impacts of Radioactive Material in Soil,* United state, Environmental Assessment and Information Sciences Division.

Zhang, L. M., Xu, y. & Jia, J. S. 2007. Analysis of earth dam failures - A database approach. *ISGSR2007 First International Symposium on Geotechnical Safety & Risk.* Tongji University, China.

Editor's note.
This paper may be referred to, in other articles, as:

Bui Quang Cuong, Zhou Yihong and Zhao Chunju: "Seepage Evaluation in Embankment Dam based on Short-term Temperature Observation and Heat Injection" *Electronic Journal of Geotechnical Engineering*, 2016 (21.26), pp 10493-10506. Available at ejge.com.